Article

Changes in Phyllosphere Microbial Communities of *Pinus tabuliformis* after Infestation by *Bursaphelenchus xylophilus*

Yong Jiang [1], Jiaying Liu [2,3], Shichu Liang [1], Wenxu Zhu [2,3] and Hui Li [2,3,*]

1 Key Laboratory of Ecology of Rare and Endangered Species and Environmental Protection, Guangxi Normal University, Ministry of Education, Guilin 541001, China
2 College of Forestry, Shenyang Agricultual University, Shenyang 110866, China
3 Research Station of Liaohe-River Plain Forest Ecosystem, Chinese Forest Ecosystem Research Network (CFERN), Shenyang Agricultural University, Tieling 112000, China
* Correspondence: lihui@syau.edu.cn; Tel.: +86-15940526007

Abstract: Phyllosphere microbial communities have an important role in plant growth and resistance to pathogen infection and are partially influenced by leaf characteristics. Pinewood nematode, Bursaphelenchus xylophilus, is one of the greatest threats to pine trees and is spreading all over the world. However, studies on the resistance of plant–microbe interactions to pathogens during the nematode's pathogenesis and the relationships of leaf chemical characteristics caused by pinewood nematode and phyllosphere microbial communities are limited. In this study, different stages of *Pinus tabuliformis* that were healthy or infected with *B. xylophilus*-associated leaf characteristics and phyllosphere bacterial and fungal communities were compared. These results demonstrated that soluble sugar and starch contents decreased based on the extent of infection. Phyllosphere microbial community changes potentially caused by *B. xylophilus* infection of *P. tabuliformis* and the fungal community compositions of healthy *P. tabuliformis* trees (Ya) were clearly different from diseased *P. tabuliformis* trees at an early stage of *B. xylophilus* infection (Yb) and *P. tabuliformis* trees in the last stage of *B. xylophilus* infection (Yc), particularly along the first coordinate axis. According to a linear discriminant effect size (LEfSe) analysis, the biomarker species in the phyllosphere of Yb were Acidobacteria, Deinococcus-Thermus, and Patescibacteria, while those in the phyllosphere of Ya were Proteobacteria, *Aureobasidium*, *Dictyosporium*, *Alternariaster*, *Knufia*, *Microstroma*, and *Naganishia*. Particularly at the end of PWD (pine wilt disease) infection, the majority of microbial taxa tended to co-exclude rather than co-occur with PWD infection. The result of a canonical correlation analysis (CCA) showed that the chemical properties of leaves, such as carbon and nitrogen, have significant impacts on phyllosphere microbial communities. These results expanded the possible connections between the phyllosphere communities and plant health.

Keywords: *Pinus tabuliformis*; phyllosphere microorganism; leaf characteristics; pine wilt disease

1. Introduction

Pinus tabuliformis is one of the dominant species used for afforestation in North China, and plantations of this species are very important for enhancing the ecological environment and for conserving soil and water [1]. Conifers in the Pinaceae family, such as pine trees, serve as important sources of forest products and provide other environmental functions such as providing wind and sand breaks, preventing landslides, and creating stunning landscapes [2]. As one of the most devastating conifer diseases in the world, pine wilt disease (PWD) is a devastating forest disease caused by the pinewood nematode (PWN) *Bursaphelenchus xylophilus,* and it can affect several species of pine trees [3,4]. PWD is spread by pine sawyer longhorn beetles, *Monochamus* spp. Relevant data showed that a variety of pine wood nematode infections not only kill trees but may also disrupt the ecological balance in the area and cause ecological problems. This could result in the loss of pine

planting, particularly in the years to come, with climate change and the anticipated rise in global temperatures [5]. If the disease cannot be detected early and effectively controlled, it could infect all the Chinese pine in the area within 3 to 5 years, which would lead to very serious economic losses in a relatively short period of time. Therefore, there is an urgent need for a continuing coordinated effort to prevent the spread of PWD [4].

Numerous studies have concentrated on the infection mechanism of PWD [6,7], the biology of *B. xylophilus* [8,9], and the insect vectors [4,10]. A recent study demonstrated that plant microbiome changes are not just a passive reaction on the part of plants but rather that, as a result of convolution, plants are likely to actively seek out cooperation with microbes to alleviate stresses [11]. Previous studies have demonstrated that a host nematode infection can have an impact on the microbial communities in the leaves of the host by causing changes in growth conditions or a decline in plant fitness (e.g., healthy status) [12–14]. *B. xylophilus* infection has been linked to changes in the diversity and organization of the bacteria that colonize the wood of *P. pinaster* trees as well as changes in the abundance of specific taxonomic groups, such as *Streptomyces* and *Pseudomonas* [15]. The intensity of pine chemical defenses and the carbohydrate concentrations of pines can be influenced by fungi and bacteria [16]. The microbes that colonize the plant can be impacted by changes in secretions [17,18]. Although the impact of phyllosphere bacteria on plants is well understood, little is known about the effect of PWD in the field on the phyllosphere microbial communities, particularly phyllosphere fungi. The nutrient compositions (carbon, phosphorus, soluble sugar, starch content, etc.) of different plant leaves affect the colonization of interleaf microorganisms [19,20]. Similar to the rhizosphere, the phyllosphere (the portion of terrestrial plants that is aboveground) is a crucial plant niche that supports a wide variety of microscopic organisms [21]. The phyllosphere is inhabited by diverse microbes, with some microbes living on the surfaces of plants as epiphytes and others colonizing inside tissues (e.g., leaves) as endophytes [22]. The bacteria, fungi, and other microscopic organisms that live on plant foliage make up the phyllosphere microbes. In the present study, the phyllosphere microorganisms of pine were focused on needles.

Numerous studies have demonstrated the abundance of phyllosphere microorganisms, which can enhance plant stress resistance and disease resistance, among other things, and play a crucial role in the stability and function of the plant ecosystem [23]. These interactions between plants and microbes are thought to be essential for preserving plant health [24]. The evidence for rhizosphere-mediated resistance to nematode infection and for maintaining plant health through microbiome regulation has grown in recent years [25,26]. There is uncertainty about whether and how phyllosphere microbiomes respond to nematode infection challenges for the benefit of the plant hosts. The discovery of the link between nematode infection and the phyllosphere microbiome response will help us understand the interactions between microbes, plants, and nematode infection and add more proof in favor of the "cry for help" strategy used by the plant holobiont. In some cases, the microbial changes may have an impact on the health and sustainability of plants [27]. In addition to diversity and community composition, microbial interactions are essential components of the microbiome, and these interactions are crucial for determining how well an ecosystem functioning [28].

Approximately 64,280 hm^2 (square hundred meter) of China were affected by pine wilt disease until 2008, and nearly 1,061,700 pines perished as a result of *B. xylophilus* infection ("Chinese green times", 21 August 2009). By 2011, the disease had spread widely throughout China, with 175 counties and 15 provinces affected by the pinewood nematode [29]. Large areas of *P. tabuliformis* are, however, stressed by pests and diseases, the most damaging of which is PWD, which is having negative effects on the environment and causing significant economic losses [30]. A thorough understanding of the microbial community structure in pine trees can lead to a better understanding of nematode infection. It also provides a scientific foundation for understanding the symbiotic relationships between the host and microorganisms as well as the development and utilization of microbial resources.

In the current study, we sequenced the 16S rRNA and ITS gene amplicons to better understand the changes in the host phyllosphere microbial communities brought on by PWD. We also built molecular ecological networks based on random matrix theory to better understand the relationships between nematode infection and host microbial communities in order to explore how the changes in phyllosphere microbial community regulate plant growth or disease resistance. The current study also lays the groundwork for investigating new prevention and control methods for pine wood nematode by illuminating the community structure of microorganisms in *P. tabuliformis* before and after the invasion of pine wood nematode.

2. Materials and Methods

2.1. Overview of the Research Area

The study area was spread across five sites in Dengta City, Liaoyang City, Liaoning Province, China (41°17′44″, 123°35′47″). With an annual average temperature of 8.8 °C, an annual average precipitation of 600 to 800 mm, and an annual average frost-free period of 140 to 160 days, this region has a northern temperate continental climate. Eutrochrepts soil is the category given to the type of soil in this region [31]. The region is 1167 square kilometers in size and is primarily covered in forest made up of *P. tabuliformis* and *P. koraiensis*, both of which are about 40 years old. Five fixed plots with areas of 1 ha and the same conditions and basic soil properties were chosen. In each plot, ten healthy trees (Ya), ten *P. tabuliformis* trees in the early stages of infection (Yb), and ten *P. tabuliformis* trees in the last stage of *B. xylophilus* infection (Yc) were selected for sampling. The distances between the diseased trees and the nearby healthy trees were less than 15 m. The method described by Millberg et al. [32] was used to choose the diseased and healthy trees, in which the healthy trees had completely green needles and no *B. xylophilus* was isolated from these trees. Trees in the early stages of infection had needles that had become slightly wilted and brown. The diseased trees looked completely dead with brown needles. The subsequent confirmation of healthy and diseased trees was performed in the lab using specific *B. xylophilus* primers and nematode isolation techniques [33].

2.2. Sample Collection

For the sampling, 30 needle samples were collected and mixed into one replicate at each site from the tips of the shoots in the middle of the canopy in three directions from 10 trees, including 120° around the tree in August 2021. In total, 15 leaf samples (3 types × 5 replicates) were taken from the study area. An ice box was used to transport all of the samples to the lab for further analysis.

To analyze the microbial communities on the leaves according to Ren et al. [34], 10 g of leaf samples from each replicate were cut into pieces and transferred to a sterile triangle flask. Then, a 1:20 (leaf weight/volume TE buffer = 1:20) phosphate-buffered saline solution (20 mL, PBS, 0.01 M, pH 7.4) was added to each triangle flask. After sealing with a sterilized film, the samples were shaken on a shaker at 200 r/min for 30 min at room temperature, and the microbial cells were separated from the leaf surface. Vacuum filtration was used in a sterile environment, and microbes from the oscillating liquid were collected on a 0.22 μm filter membrane, placed into 2 mL sterile centrifuge tubes, and stored at −80 °C prior to DNA extraction and high-throughput sequencing.

The leaves were then rinsed and dried off from the sterile triangle flask. To analyze the leaf characteristics, the leaves were dried at 105 °C for 30 min and then at 65 °C to a constant weight.

2.3. Determination of Leaf Characteristics

The dried plant samples were pulverized and passed through a 100-mesh sieve. The 3.5–4.2 mg leaf samples were weighed in a tin cup (3 mm × 5 mm), wrapped, and placed in an autosampler. The total carbon and nitrogen contents in leaves were analyzed with oxidation–combustion gas chromatography using an elemental analyzer (vario MACRO

cube). A 1 g sample was weighed in a 10 mL centrifuge tube and 8 mL of an 80% ethanol solution was added for 30 min at 80 °C, cooled, and centrifuged, which was repeated three times. The soluble sugar and starch were determined following the enthrone calorimetric method.

2.4. DNA Extraction, Amplification of the 16S rDNA Region, and Illumina MiSeq Sequencing

The Fast DNA SPIN Kit for soil (MP Biomedicals, Santa Ana, CA, USA) was used to extract genomic DNA from a filter membrane in accordance with the manufacturer's instructions. A NanoDrop ND-1000 spectrophotometer (Thermo Fisher Scientific, Waltham, MA, USA) was used to measure the DNA concentrations. Using the primer pairs 338F (5′-ACTCCTACGGGAGGCAGCAG-3′) and 806R (5′-GGACTACHVGGGTWTCTAAT-3′) with a barcode sequence, the V3-V4 regions of the bacterial 16S rDNA gene were amplified and sequenced. Using the primer pairs ITS1F (5′-CTTGGTCATTTAGAGGAAGTAA-3′) and ITS2R (5′-GCTGCGTTCTTCATCGATGC-3′) with a barcode sequence, the ITS1 regions of the fungal ITS rDNA gene were amplified [35]. All of the PCR reactions used a 25 µL mixture that included 8.75 µL of ddH$_2$O, 1 µL (10 uM) of forward primer and reverse primer, 2 µL of dNTPs (2.5 mM) and DNA template (40–50 ng), 0.25 µL (5 U/µL) of Q5 High-Fidelity DNA Polymerase, and 5 µL of Q5 High-Fidelity GC buffer (5×) and Q5 reaction buffer (5×). An initial step of denaturation at 98 °C for 5 min was followed by 25 cycles of denaturation at 98 °C for 15 s, annealing at 55 °C for 30 s, and elongation at 72 °C for 30 s, with a final elongation step of 5 min at 72 °C. PCR amplicons were further purified and quantified with the help of Agencourt AMPure Beads (Beckman Coulter, Indianapolis, IN, USA) and a PicoGreen dsDNA Assay Kit (Invitrogen, Carlsbad, CA, USA). Shanghai Personal Biotechnology Co., Ltd., Shanghai, China used an Illumina MiSeq PE300 platform to sequence PCR products. The NCBI database SRA accession number for of the raw high-throughput sequencing data of the phyllosphere and rhizosphere bacteria and fungi is PRJNA688988.

2.5. Bioinformatics and Statistical Analysis

High-quality sequences were eventually obtained after the primers and barcode sequences were removed using cutadapt, quality filter, denoise, joint, and the removal of chimeras. Sequences with an average similarity of ≥97% were grouped under one OTU. Each representative sequence was taken from the Silva Database for bacteria (Release 132, http://www.arb-silva.de; accessed on 1 November 19) [36] and Unite Database for fungi (Release 8.0, https://unite.ut.ee/; accessed on 1 November 19) [37]. To find differences in community richness (Chao 1 and observed species), diversity (Shannon and Simpson), and evenness (Pielou_e) among treatments, one-way analyses of variance (ANOVA) with LSD tests were used. Phyllosphere microbial community diversity and leaf characteristic relationships were examined using Spearman's rank correlation. Using RStudio's vegan package, Venn diagrams were created using subsample data to display shared and unique OTUs. To determine the bacterial and fungal taxonomic levels (from phylum to genus) responsible for the community differentiation between treatments, an LEfSe with a Kruskal–Wallis test was used [38]. The logarithmic LDA threshold was set at 2.48 for discriminative features. In order to see the structure of the microbial communities, an NMDS analysis with Jaccard distances was used to estimate the microbial beta-diversity. Utilizing a network analysis with Rstudio's "psych" package based on Spearman's rank correlation, the co-occurrence patterns of ASVs from various treatments were assessed. Gephi software was used to visualize the networks using a Fruchterman–Reingold layout. The influence of leaf characteristics on the composition of the phyllosphere microbial community was clarified using a canonical correlation analysis (CCA).

3. Results

3.1. Leaf Characteristics between Diseased and Healthy Trees

No significant differences in the TC and TN concentrations or C/N were obtained among the different samples. The observed soluble sugar and starch storage of the leaves varied from 45.20 mg/g and 35.05 mg/g in Yc to 83.97 mg/g and 65.85 mg/g in Ya. The soluble sugar and starch contents among different samples decreased based on the extent of infection (Table 1).

Table 1. Plant leaf characteristics between diseased and healthy trees.

	TC (g·kg^{-1})	TN (g·kg^{-1})	C/N	Soluble Sugar (mg·g^{-1})	Starch (mg·g^{-1})
Ya	17.71 ± 0.77 [a]	554.31 ± 11.49 [a]	31.52 ± 1.36 [a]	83.97 ± 3.58 [a]	65.85 ± 4.40 [a]
Yb	17.39 ± 0.48 [a]	545.56 ± 1.24 [ab]	31.47 ± 0.85 [a]	65.27 ± 1.95 [b]	41.93 ± 5.83 [b]
Yc	16.94 ± 0.73 [a]	532.81 ± 2.71 [b]	31.70 ± 1.49 [a]	45.20 ± 2.37 [c]	35.05 ± 3.28 [b]
F value	0.32	2.49	0.01	50.82	12.24
p value	0.73	0.12	0.99	<0.01	<0.01

Means ± standard errors. Different lower-case letters in the same column indicate significant differences at $p < 0.05$. TC: total carbon; TN: total nitrogen; Ya: healthy *Pinus tabuliformis* trees; Yb: diseased *P. tabuliformis* trees at an early stage of *B. xylophilus* infection; Yc: diseased *P. tabuliformis* trees in the last stage.

3.2. Phyllosphere Microbial Community Diversity between Healthy and Diseased Trees

In total, 1,281,396 and 1,133,002 high-quality bacterial and fungal sequences were obtained from all samples, allowing us to further explore the bacterial and fungal communities. The average numbers of bacterial and fungal sequences per sample were 85,426 and 75,533, respectively, ranging from 72,698 to 113,244 and from 49,753 to 97,382 per sample. All sequences were assigned to 17,658 bacterial ASVs and 1582 fungal ASVs. The number of shared phyllosphere bacterial OTUs among Ya, Yb, and Yc was 1213, and the numbers of unique OTUs of Ya, Yb, and Yc were 3270, 4760, and 6054, respectively (Figure 1A). In addition, the number of shared phyllosphere fungal OTUs among Ya, Yb, and Yc was 207, and the numbers of unique OTUs of Ya, Yb, and Yc were 253, 466, and 322, respectively (Figure 1B).
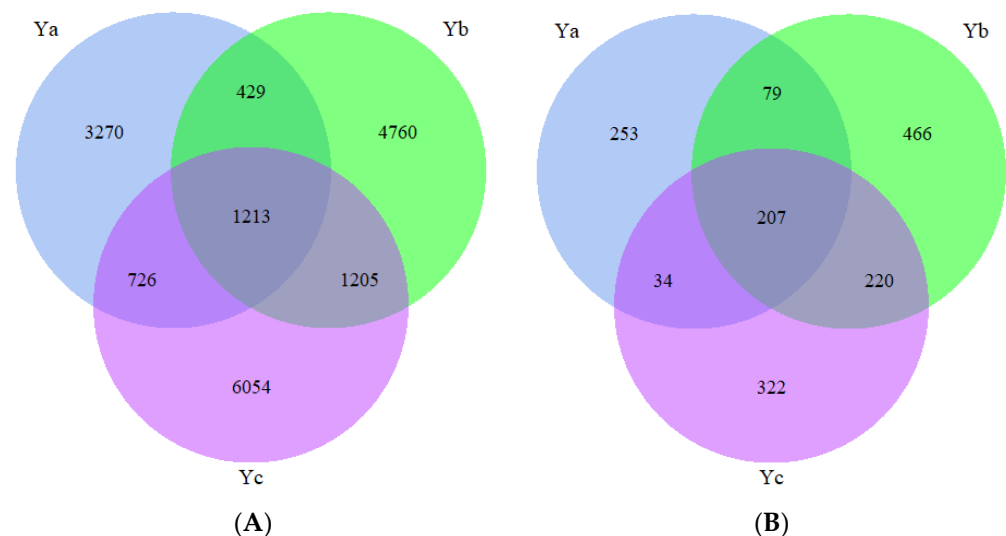
Figure 1. The shared and unique OTUs of phyllosphere bacteria (**A**) and fungi (**B**). Ya: healthy *Pinus tabuliformis* trees; Yb: diseased *P. tabuliformis* trees at an early stage of *B. xylophilus* infection; Yc: diseased *P. tabuliformis* trees in the last stage.

There was considerable variation in the phyllosphere bacterial Chao 1 index (F = 12.53, $p < 0.01$), Good's coverage (F = 15.67, $p < 0.01$) and observed species (F = 10.72, $p < 0.01$)

among Ya, Yb, and Yc (Table 2). The Chao 1 index was the highest in Yc, at 3254.42, significantly higher than those of Yb and Ya, and lowest in Ya, at 1783.20. The Shannon index was the highest in Yc, at 7.85, followed by Yb, and was lowest in Ya, at 6.33 (Table 2). Meanwhile, no obvious differences in the Pielou e index (F = 1.78, p = 0.21), Shannon index (F = 3.15, p = 0.08), and Simpson index (F = 0.36, p = 0.71) were obtained among Ya, Yb, and Yc. With regard to phyllosphere fungal community diversity, the Chao 1 index (F = 14.19, p < 0.01), observed species (F = 16.71, p < 0.01), Pielou e index (F = 10.56, p < 0.01), Shannon index (F = 15.03, p < 0.01), and Simpson index (F = 4.15, p = 0.04) presented significant differences among Ya, Yb, and Yc. It is interesting to note that the Chao 1 index, Pielou e index, Shannon index, and Simpson index of Yb were the highest, at 427.15, 418.90, 0.66, 5.77, and 0.94, respectively, followed by Yc and Ya (Table 2).

Table 2. Phyllosphere bacterial and fungal community diversity among Ya, Yb, and Yc.

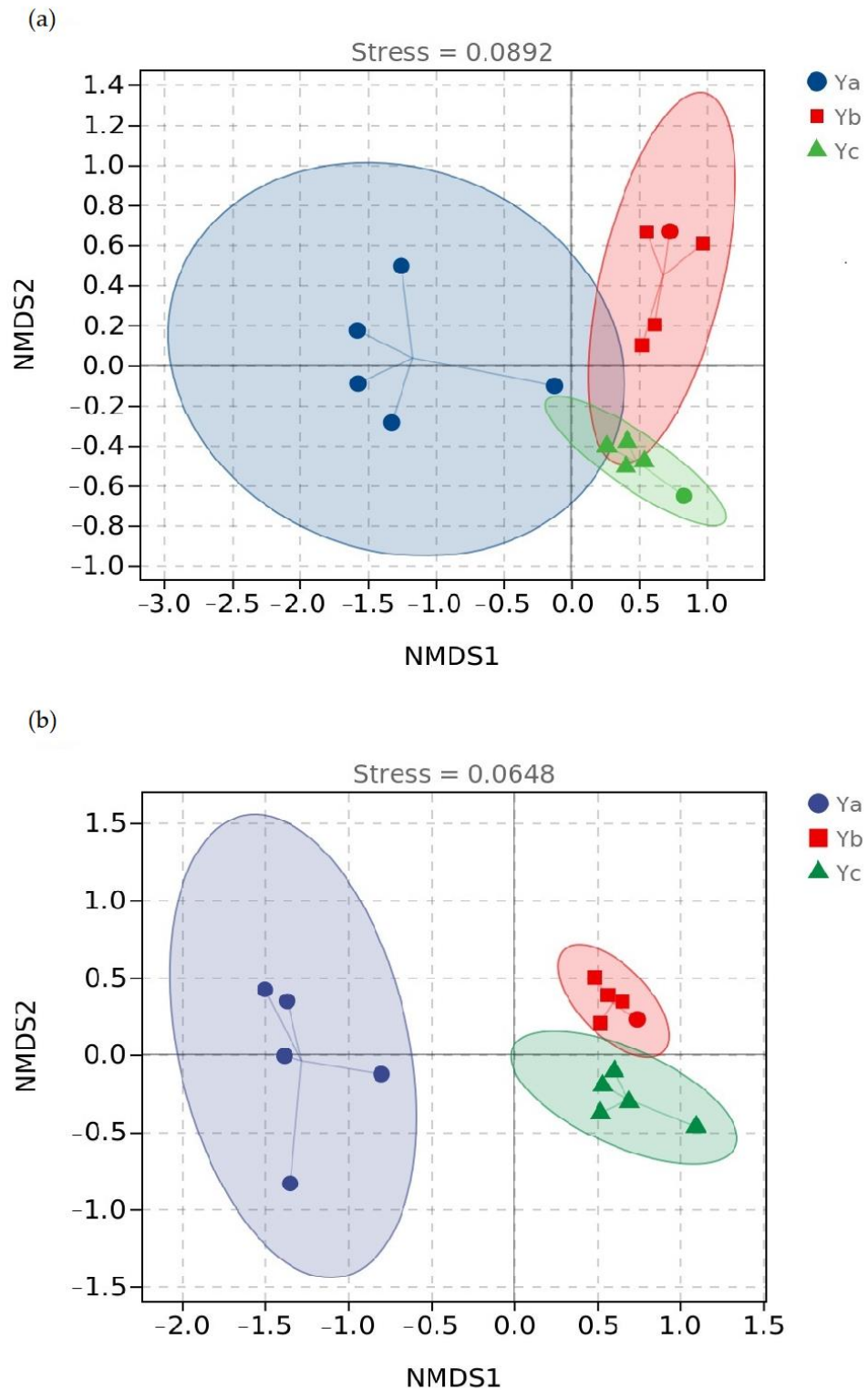| Phyllosphere Bacterial Community Diversity	Ya	Yb	Yc	F	p
Chao 1 index	1783.20 ± 683.14 [b]	2842.11 ± 388.24 [a]	3254.42 ± 268.42 [a]	12.53	<0.01
Good's coverage	0.995 ± 0.002 [a]	0.992 ± 0.001 [b]	0.991 ± 0.001 [b]	15.67	<0.01
Observed species	1636.98 ± 644.96 [b]	2527.68 ± 396.60 [a]	2972.96 ± 272.61 [a]	10.72	<0.01
Pielou e index	0.59 ± 0.10 [a]	0.65 ± 0.06 [a]	0.68 ± 0.06 [a]	1.78	0.21
Shannon index	6.33 ± 1.33 [b]	7.34 ± 0.74 [ab]	7.85 ± 0.73 [a]	3.15	0.08
Simpson index	0.940 ± 0.051 [a]	0.962 ± 0.030 [a]	0.958 ± 0.043 [a]	0.36	0.71
Phyllosphere Fungal Community Diversity	**Ya**	**Yb**	**Yc**	**F**	**p**
Chao 1 index	232.72 ± 45.25 [b]	427.15 ± 90.10 [a]	357.30 ± 9.34 [a]	14.19	<0.01
Good's coverage	0.9996 ± 0.0002 [a]	0.9996 ± 0.0004 [a]	0.9995 ± 0.0001 [a]	0.38	0.69
Observed species	226.50 ± 43.44 [b]	418.90 ± 80.75 [a]	348.32 ± 9.81 [a]	16.71	<0.01
Pielou e index	0.50 ± 0.09 [b]	0.66 ± 0.02 [a]	0.61 ± 0.04 [a]	10.56	<0.01
Shannon index	3.93 ± 0.79 [b]	5.77 ± 0.35 [a]	5.12 ± 0.36 [a]	15.03	<0.01
Simpson index	0.85 ± 0.09 [b]	0.94 ± 0.02 [a]	0.92 ± 0.02 [ab]	4.15	0.04

Means ± standard errors. Different lower-case letters in the same row indicate significant differences at p < 0.05. Ya: healthy *Pinus tabuliformis* trees; Yb: diseased *P. tabuliformis* trees at an early stage of *B. xylophilus* infection; Yc: diseased *P. tabuliformis* trees in the last stage.

In addition, we comprehensively profiled the phyllosphere microbial community beta diversity, and an NMDS analysis based on the Jaccard distances revealed that the phyllosphere fungal compositions of Ya, Yb, and Yc formed three distinct clusters and the fungal community composition of Ya was clearly distinguished from Yb and Yc, especially along the first coordinate axis (Figure 2).

3.3. Phyllosphere Microbial Community Composition between Healthy and Diseased Trees

Across all samples, we obtained 29 bacterial phyla and 519 bacterial genera. At the phylum level, nine bacterial communities, including Proteobacteria, Bacteroidetes, Actinobacteria, Acidobacteria, Deinococcus-Thermus, Firmicutes, Patescibacteria, Armatimonadetes, and Planctomycetota, with relative abundances greater than 0.1% were detected (Figure 3A). The relative abundance of Proteobacteria was the highest in Ya, at 93.43%. When *P. tabuliformis* was infected with the pine wood nematode, the relative abundance of Proteobacteria decreased dramatically (Figure 3A). At the genus level, the phyllosphere bacterial communities with relative abundances of more than 1% were *Pantoea*, *Acinetobacter*, *Sphingomonas*, *Methylobacterium*, *Pseudomonas*, *Kosakonia*, *Hymenobacter*, *Massilia*, *Stenotrophomonas*, *Chryseobacterium*, and *Amnibacterium* (Figure 3B). A heatmap shows that the phyllosphere bacterial communities among Ya, Yb, and Yc clearly differed (Figure 4A). The relative abundances of *Sphingobacterium*, *Pedobacter*, *Kosakonia*, and *Acinetobacter* were the highest in Yc, and *Psychroglaciecola* and *Variovarax* were the larger groups in Ya. Moreover, the relative abundances of *Actinoplanes* and *Acidiphilium* were greater in Yb (Figure 4A). Additionally, we used an LEfSe analysis to determine which microbial taxa (from the phy-

lum level to the genus level) were the primary causes of the variations in community compositions among Ya, Yb, and Yc (Figure 5A). At the bacterial phylum level, the larger groups of bacteria in Yb were Acidobacteria, Deinococcus-Thermus, and Patescibacteria, while in Ya the larger group was Proteobacteria (Kruskal–Wallis test, $p < 0.01$) (Figure 5A).

(a)

(b)

Figure 2. NMDS analysis based on Jaccard distances of phyllosphere bacterial (**a**) and fungal (**b**) community compositions among Ya, Yb, and Yc. Ya: healthy *Pinus tabuliformis* trees; Yb: diseased *P. tabuliformis* trees at an early stage of *B. xylophilus* infection; Yc: diseased *P. tabuliformis* trees in the last stage.

Additionally, for fungi, in total, 6 dominant fungal phyla and 335 fungal genera were detected, including Ascomycota, Basidiomycota, Chytridiomycota, Mucoromycota, Mortierellomycota, and Rozellomycota, of which Ascomycota was the predominant fungal community, with an average relative abundance of 71.9%, followed by Basidiomycota (Figure 3C). The fungal group of Ascomycota was significantly enriched in Ya, at 83.48%, compared to Yb and Yc. Meanwhile, Yc contained significantly higher abundances of Basidiomycota and Chytridiomycota than Ya and Yb (Figure 3C). At the genus level, phyllosphere fungal communities with relative abundances of more than 1% were *Alternaria*, *Didymella*, *Farysizyma*, *Selenophoma*, *Strelitziana*, *Aureobasidium*, *Naganishia*, *Phialemoniopsis*, *Septoria*, *Genolevuria*, *Gibberella*, *Trichomerium*, and *Paraphaeosphaeria* (Figure 3D). A heatmap based on Bray–Curtis distances demonstrated that the phyllosphere fungal communities from Ya significantly differed from those of Yb and Yc (Figure 4B). The relative abundances of *Dioszegia*, *Symmetrospora*, *Cystobasidium*, and *Septoriaides* were the highest in Yc, and *Artrocatena*, *Paraconiothyrium,* and *Gibberella* were the larger groups in Ya. Moreover, the relative abundances of *Knufia* and *Vishniacozyma* were greater in Yb (Figure 4B). An LEfSe analysis indicated that the larger group of fungi in Yc was Farysizyma, while in Ya the larger groups were Buckleyzymaceae, Phialemoniopsis, and Pseudorobillarda (Kruskal–Wallis test, $p < 0.01$) (Figure 5B). At the fungal genus level, the larger groups of fungi in Yc were *Septoria*, *Devriesia*, *Truncatella*, and *Pestalotiopsis*, while in Ya the larger groups were *Aureobasidium*, *Dictyosporium*, *Alternariaster*, *Knufia*, *Microstroma*, and *Naganishia* (Kruskal–Wallis test, $p < 0.01$) (Figure 5B).
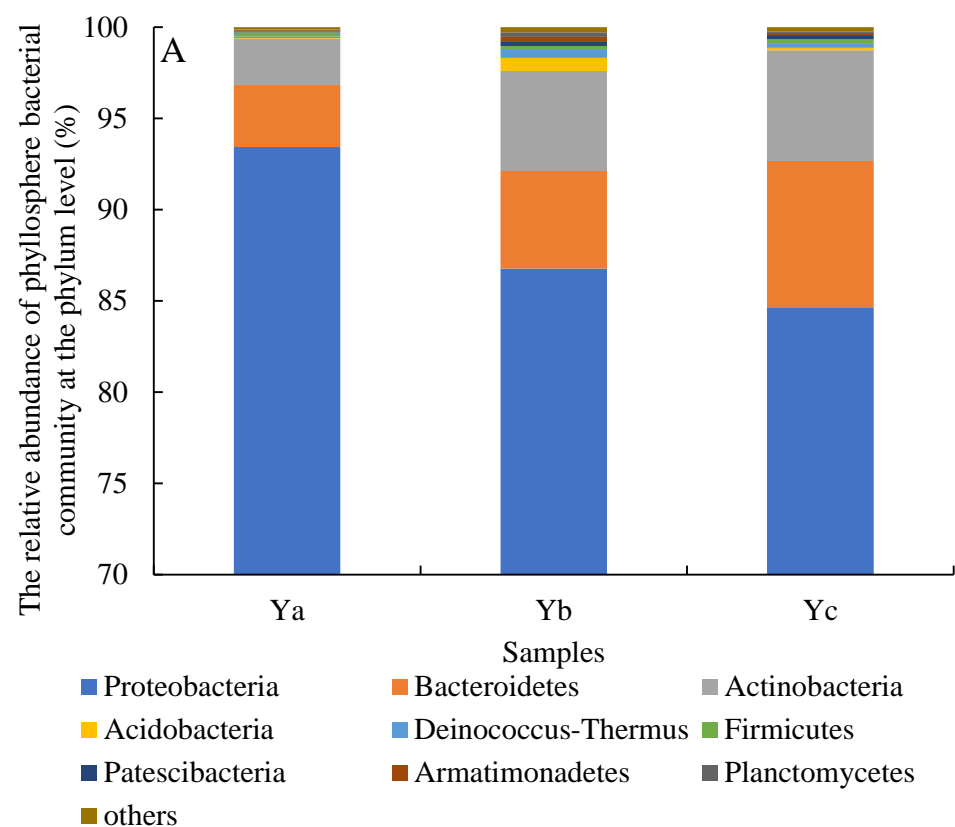
Figure 3. *Cont.*
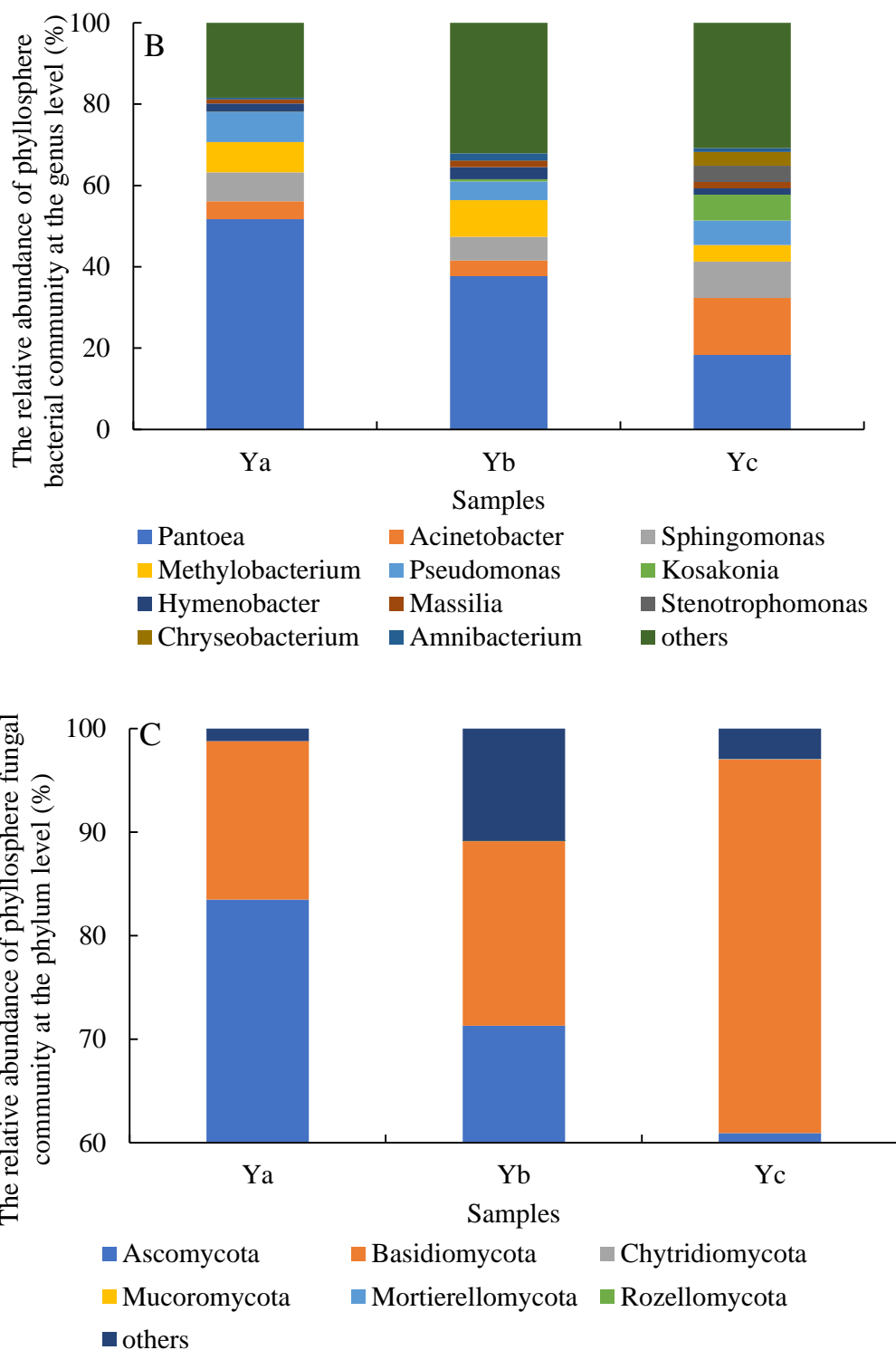
Figure 3. *Cont.*
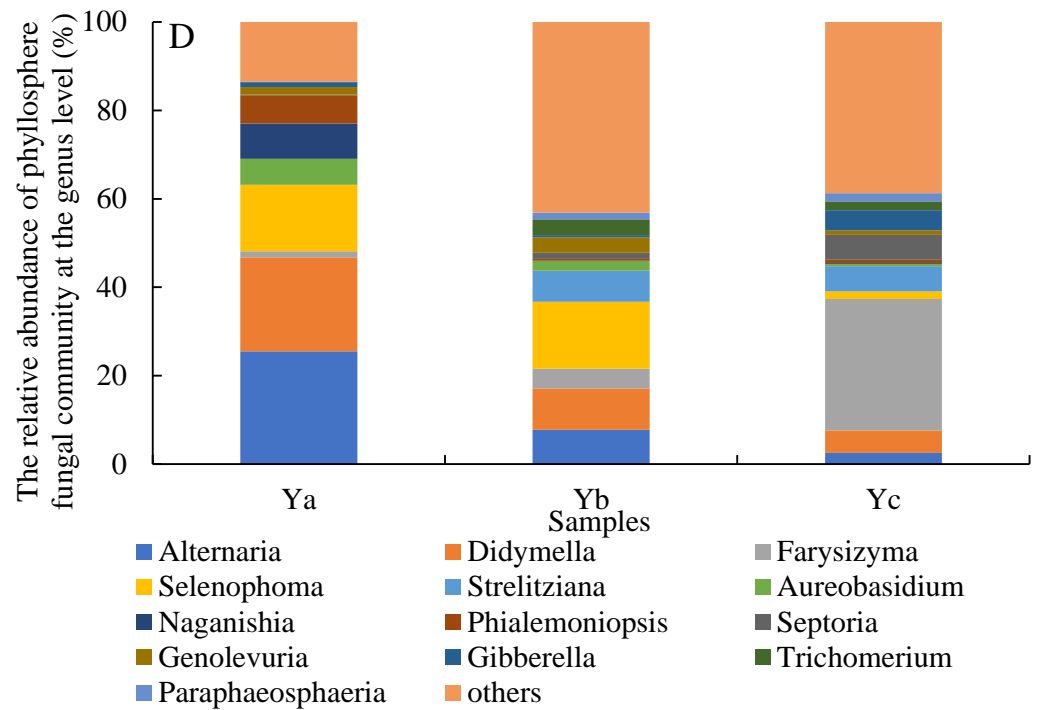
Figure 3. The relative abundances of phyllosphere bacterial (**A**,**B**) and fungal (**C**,**D**) community compositions at the phylum and genus levels. Different lower-case letters in the same row indicate significant differences at $p < 0.05$. Ya: healthy *Pinus tabuliformis* trees; Yb: diseased *P. tabuliformis* trees at an early stage of *B. xylophilus* infection; Yc: diseased *P. tabuliformis* trees in the last stage.

(**A**)
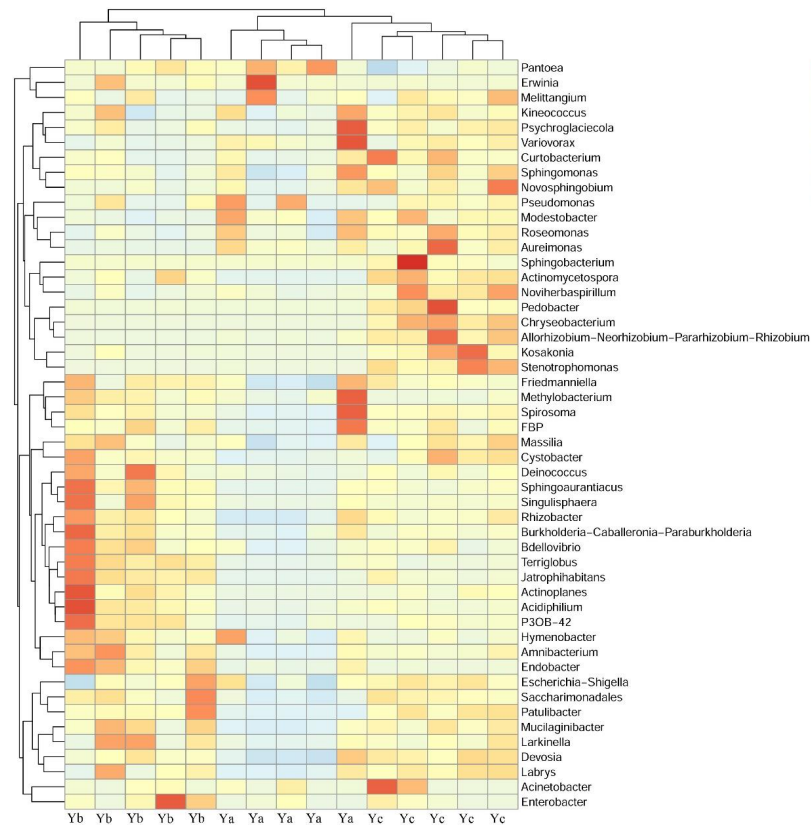
Figure 4. *Cont.*
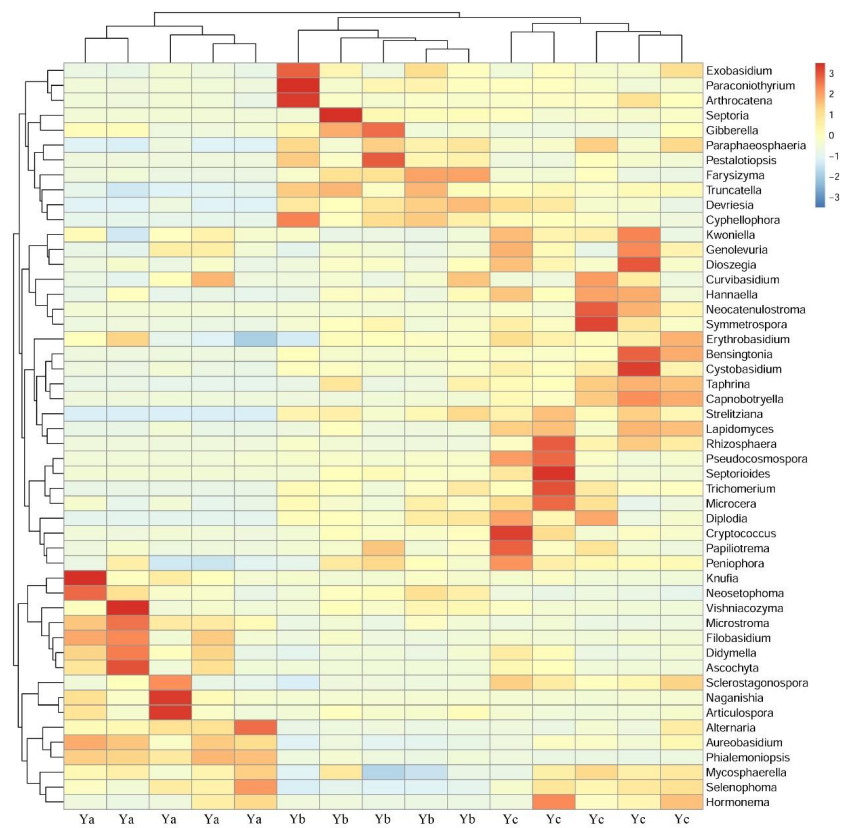
(**B**)

Figure 4. Heatmaps of the top 50 phyllosphere bacterial (**A**) and fungal (**B**) communities at the genus level. The scale "−3 to +3" refers to the relative abundance of the corresponding taxonomic unit in each sample/group of the grouping scheme. Ya: healthy *Pinus tabuliformis* trees; Yb: diseased *P. tabuliformis* trees at an early stage of *B. xylophilus* infection; Yc: diseased *P. tabuliformis* trees in the last stage.

3.4. Bacterial and Fungal Co-Occurrence Networks, as Affected by Bursaphelenchus xylophilus Infection

We developed association networks of phyllosphere bacterial and fungal communities from ASV data to further disentangle the complex microbial interactions (Figure 6; Table S1). Phyllosphere bacterial networks had fewer positive correlations than fungal networks and had more negative correlations than fungal networks. The lower aggregation coefficients of phyllosphere bacterial and fungal networks with *B. xylophilus* infection indicated a lower degree of modularity of the co-occurrence networks. Positive links showed decreases with the infection of PWD, and in the last stage the positive links were the lowest (Figure 6; Table S1), demonstrating that most of the microbial taxa tended to be co-excluding rather than co-occurring. The positive correlation of bacterial and fungal networks decreased and the negative correlation increased in the early and late stages of nematode infection. The graph density of phyllosphere bacteria in the network of Yb, a key topological property to describe how well a node is connected with its neighbors, was higher than the graph density values of Ya and Yc, suggesting more intensive microbial coupling at the early stage of infection (Figure 6; Table S1).

(A)

The current LDA threshold is 2.48

■ Ya ■ Yb ■ Yc

a: p__Acidobacteria
b: p__Deinococcus_Thermus
c: p__Patescibacteria
d: p__Proteobacteria
e: c__Acidobacteria
f: c__Subgroup_6
g: c__Thermoleophilia
h: c__Deinococci
i: c__Bacilli
j: c__Saccharimonadia
k: c__Deltaproteobacteria
l: o__Acidobacteriales
m: o__Subgroup_6
n: o__Micromonosporales
o: o__Propionibacteriales
p: o__Pseudonocardiales
q: o__Solirubrobacterales
r: o__Flavobacteriales
s: o__Sphingobacteriales
t: o__Deinococcales
u: o__Bacillales
v: o__Saccharimonadales
w: o__Acetobacterales
x: o__Caulobacterales
y: o__Rhodobacterales

z: o__Bdellovibrionales
a1: o__Myxococcales
b1: o__Xanthomonadales
c1: f__Caulobacteraceae
d1: f__Subgroup_6
e1: f__Frankiaceae
f1: f__Nakamurellaceae
g1: f__Micromonosporaceae
h1: f__Nocardioidaceae
i1: f__Pseudonocardiaceae
j1: f__Solirubrobacteraceae
k1: f__Weeksellaceae
l1: f__Sphingobacteriaceae
m1: f__Deinococcaceae
n1: f__Saccharimonadales
o1: f__Acetobacteraceae
p1: f__Labraceae
q1: f__Rhizobiaceae
r1: f__Rhodobacteraceae
s1: f__Bdellovibrionaceae
t1: f__P3OB_42
u1: f__Phaselicystidaceae
v1: f__Polyangiaceae
w1: f__Chitinibacteraceae
x1: f__Neisseriaceae

y1: f__Rhodanobacteraceae
z1: f__Xanthomonadaceae
a2: g__Bryocella
b2: g__Edaphobacter
c2: g__Granulicella
d2: g__Terriglobus
e2: g__Subgroup_6
f2: g__Jatrophihabitans
g2: g__Nakamurella
h2: g__Amnibacterium
i2: g__Actinoplanes
j2: g__Marmoricola
k2: g__Nocardioides
l2: g__Actinomycetospora
m2: g__Patulibacter
n2: g__Solirubrobacter
o2: g__Dyadobacter
p2: g__Huanghella
q2: g__Chryseobacterium
r2: g__Mucilaginibacter
s2: g__Pedobacter
t2: g__Sphingobacterium
u2: g__Deinococcus
v2: g__Saccharimonadales
w2: g__Acidiphilium

x2: g__Endobacter
y2: g__1174_901_12
z2: g__Labrys
a3: g__Allorhizobium_Neorhizobium_Pararhizobium_Rhizobium
b3: g__Aureimonas
c3: g__Rubellimicrobium
d3: g__Rhizorhapis
e3: g__Sphingoaurantiacus
f3: g__Bdellovibrio
g3: g__Cystobacter
h3: g__P3OB_42
i3: g__Phaselicystis
j3: g__Pajaroellobacter
k3: g__Limnobacter
l3: g__Noviherbaspirillum
m3: g__Pelomonas
n3: g__Variovorax
o3: g__Amantichitinum
p3: g__Neisseria
q3: g__Kosakonia
r3: g__Pantoea
s3: g__Chromohalobacter
t3: g__Luteibacter
u3: g__Stenotrophomonas

(B)

The current LDA threshold is 2.84

■ Ya ■ Yb ■ Yc

a: p__Farysizyma
b: p__Buckleyzymaceae
c: p__Phialemoniopsis
d: p__Pseudorobillarda
e: p__Selenophoma
f: p__Strelitziana
g: p__Symmetrosporaceae
h: c__Pucciniomycetes
i: c__Phialemoniopsis_curvata
j: c__Pseudorobillarda_phragmitis
k: c__Selenophoma_mahoniae
l: c__Strelitziana_australiensis
m: c__Strelitziana_eucalypti
n: c__Symmetrospora
o: c__Dothideomycetes
p: c__Eurotiomycetes
q: c__Sordariomycetes
r: c__Taphrinomycetes
s: c__Agaricomycetes
t: c__Agaricostilbomycetes
u: c__Cystobasidiomycetes
v: c__Buckleyzyma
w: o__Buckleyzyma_aurantiaca
x: o__Botryosphaeriales
y: o__Capnodiales

z: o__Dothideales
a1: o__Pleosporales
b1: o__Chaetothyriales
c1: o__Thelebolales
d1: o__Hypocreales
e1: o__Trichosphaeriales
f1: o__Xylariales
g1: o__Taphrinales
h1: o__Cantharellales
i1: o__Agaricostilbales
j1: o__Erythrobasidiales
k1: o__Microstromatales
l1: o__Filobasidiales
m1: f__Chaetothyriaceae
n1: f__Pseudeurotiaceae
o1: f__Trichosphaeriaceae
p1: f__Ceratobasidiaceae
q1: f__Botryosphaeriaceae
r1: f__Mycosphaerellaceae
s1: f__Teratosphaeriaceae
t1: f__Aureobasidiaceae
u1: f__Dothideaceae
v1: f__Dictyosporaceae
w1: f__Didymosphaeriaceae
x1: f__Pleosporaceae

y1: f__Cyphellophoraceae
z1: f__Trichomeriaceae
a2: f__Hyaloscyphaceae
b2: f__Nectriaceae
c2: f__Bartaliniaceae
d2: f__Sporocadaceae
e2: f__Taphrinaceae
f2: f__Auriculariaceae
g2: f__Kondoaceae
h2: f__Erythrobasidiaceae
i2: f__Microstromataceae
j2: f__Filobasidiaceae
k2: f__Rhynchogastremataceae
l2: f__Tremellaceae
m2: f__Diplodia
n2: g__Septoria
o2: g__Capnobotryella
p2: g__Devriesia
q2: g__Lapidomyces
r2: g__Neocatenulostroma
s2: g__Aureobasidium
t2: g__Rhizosphaera
u2: g__Pyrenochaeta
v2: g__Dictyosporium
w2: g__Paraconiothyrium

x2: g__Paraphaeosphaeria
y2: g__Alternariaster
z2: g__Allophaeosphaeria
a3: g__Neosetophoma
b3: g__Alternaria
c3: g__Comoclathris
d3: g__Cyphellophora
e3: g__Knufia
f3: g__Trichomerium
g3: g__Cistella
h3: g__Fusarium
i3: g__Gibberella
j3: g__Pseudocosmospora
k3: g__Truncatella
l3: g__Pestalotiopsis
m3: g__Taphrina
n3: g__Auricularia
o3: g__Bensingtonia
p3: g__Erythrobasidium
q3: g__Microstroma
r3: g__Naganishia
s3: g__Dioszegia
t3: g__Hannaella
u3: g__Papiliotrema
v3: g__Cryptococcus

Figure 5. An LEfSe (LDA effect size) linear discriminant analysis was used to identify the biomarkers with significant differences among Ya, Yb, and Yc. From phylum to genus (from inner circle to outer circle), the taxonomic branching illustrates the taxonomic hierarchies of the main taxa in the sample community. The sizes of the nodes correspond to each taxon's average relative abundance. Nodes with different colors (green and red) indicate that those taxa exhibited significant intergroup differences and were more prevalent in the group samples represented by those colors. Hollow nodes represent taxa that did not differ significantly between groups. Letters identify the names of taxa that differed significantly between groups. (**A**): Bacteria; (**B**): Fungi. Ya: healthy *Pinus tabuliformis* trees; Yb: diseased *P. tabuliformis* trees at an early stage of *B. xylophilus* infection; Yc: diseased *P. tabuliformis* trees in the last stage.
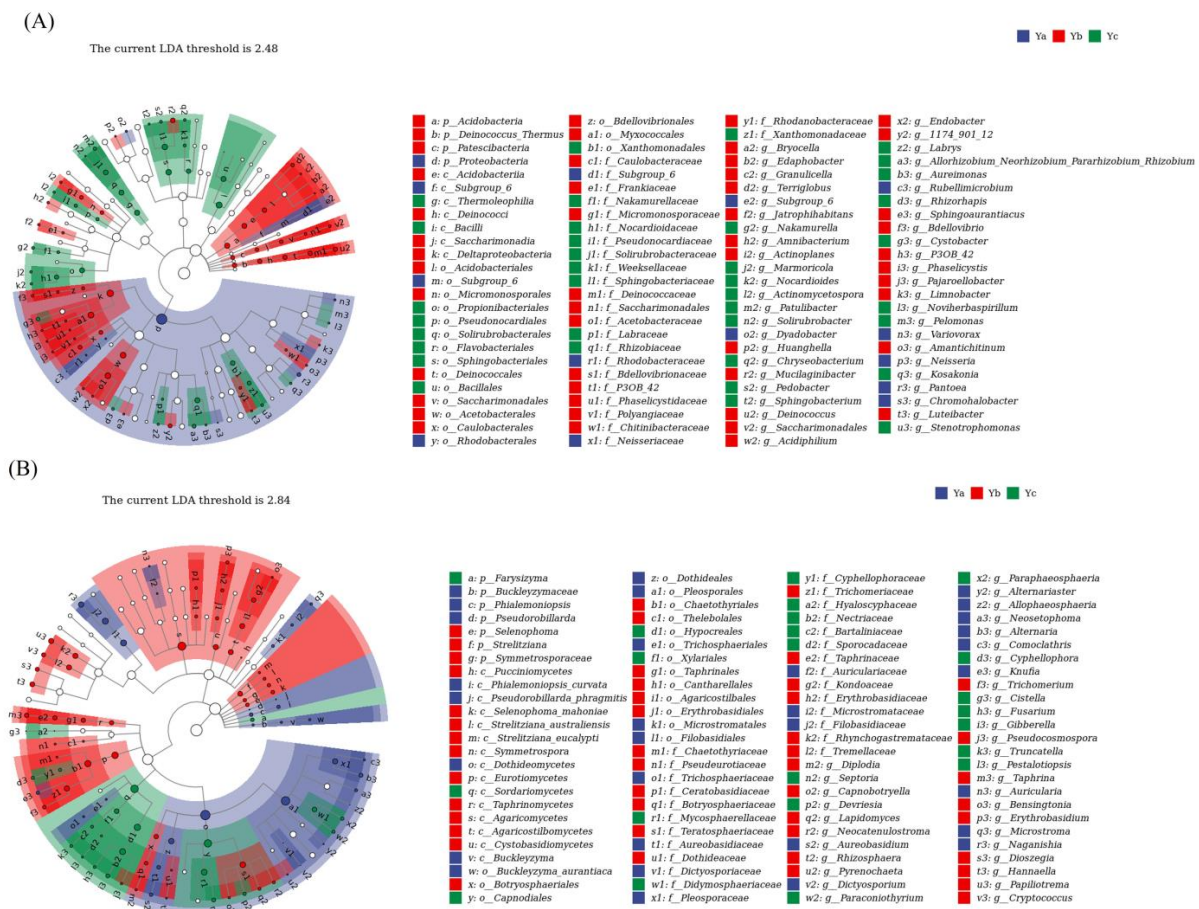
3.5. Linking Leaf Characteristics and Phyllosphere Microorganisms

The phyllosphere bacterial Chao 1 index (r = −0.86, $p < 0.01$), observed species (r = −0.83, $p < 0.01$), and Shannon index (r = −0.55, $p < 0.05$) decreased with increases in soluble sugar. In addition, the Chao 1 index had a significantly negative relation with starch (r = −0.55, $p < 0.01$). In contrast, Good's coverage index was significantly and positively correlated with the soluble sugar content (r = 0.81, $p < 0.01$) and starch content (r = 0.52, $p < 0.05$) (Table 3). The CCA results demonstrated that TC, TN, C/N, starch, and soluble sugar played important roles in shaping the phyllosphere microbial communities (Figure 7). In terms of phyllosphere bacterial and fungal community composition, CCA1 explained 33.65% and 50.44% of the five variables among individuals and was related to soluble sugar. The second principal component (CCA2) explained 23.22% and 21.66% of the total variation in the five variables, giving cumulative contribution rates accounting for 56.87% and 72.10% of variability (Figure 7). We observed Yc at the right of CCA1, associated with lower soluble sugar, starch, TC, and TN, and Ya at the left CCA1, related to higher soluble

sugar, starch, TC, and TN. In addition, the phyllosphere fungal communities were divided into three clusters, especially along CCA1 (Figure 7B).


(a)

(b)

Ya

Yb

Yc
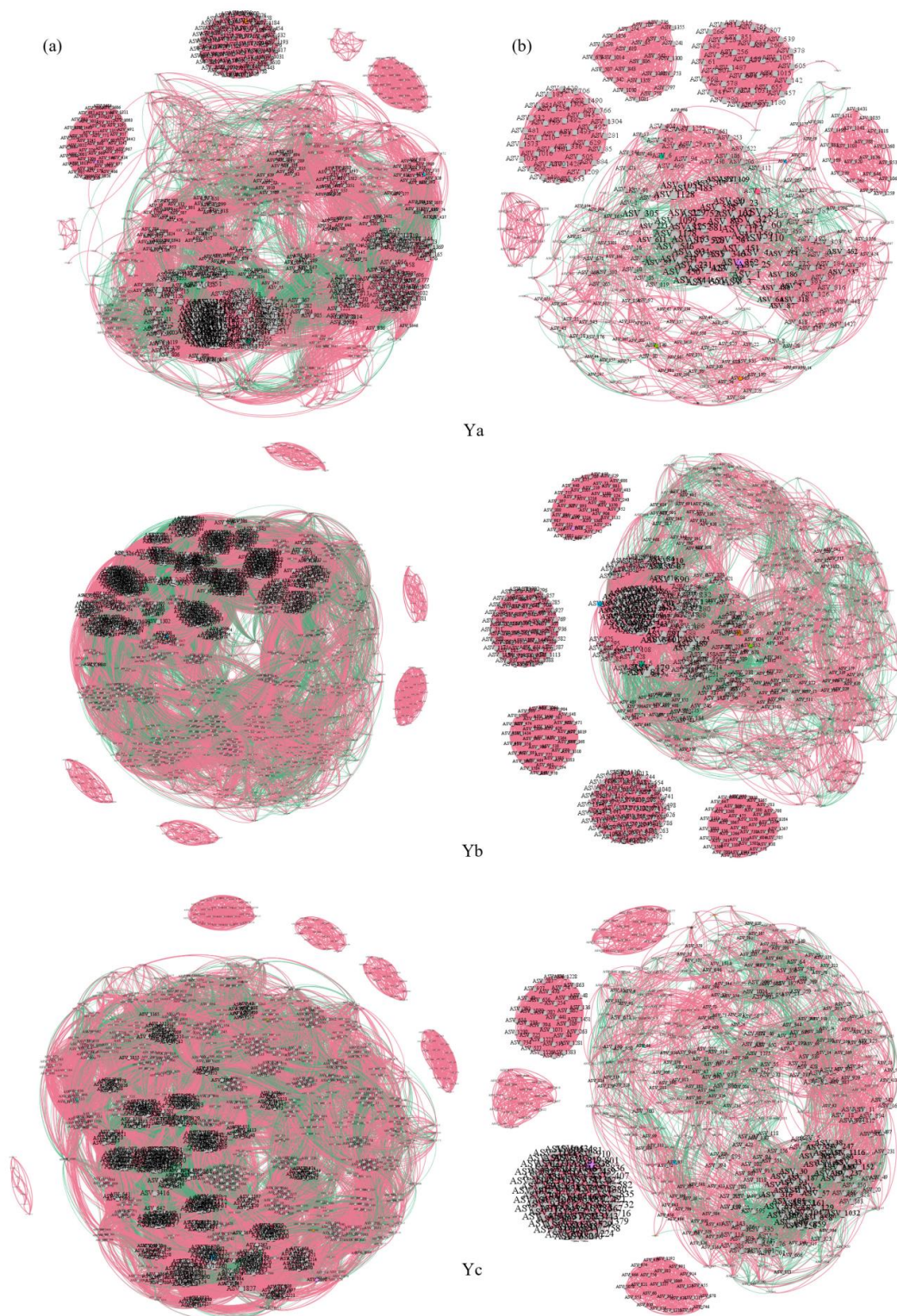
Figure 6. Network interactions of phyllosphere bacterial (**a**) and fungal (**b**) OTUs. Each node represents an OTU, and the colors of the nodes indicate different phyla. The OTUs were separated into different modules, shown as circles, by the greedy modularity optimization method. Ya: healthy *Pinus tabuliformis* trees; Yb: diseased *P. tabuliformis* trees at an early stage of *B. xylophilus* infection; Yc: diseased *P. tabuliformis* trees in the last stage.

Table 3. The relationships between leaf characteristics and phyllosphere microbial community diversity.

Bacteria	Soluble Sugar	Starch	TC	TN	C/N
Chao 1 index	−0.86 **	−0.55 *	0.05	−0.42	−0.19
Good's coverage	0.81 **	0.52 *	−0.06	0.28	0.21
Observed species	−0.83 **	−0.50	0.01	−0.44	−0.18
Pielou e index	−0.49	−0.40	0.11	−0.30	−0.23
Shannon	−0.55 *	−0.44	0.10	−0.30	−0.23
Simpson	−0.40	−0.36	−0.03	−0.33	−0.10
Fungi	**Soluble Sugar**	**Starch**	**TC**	**TN**	**C/N**
Chao 1	0.34	0.17	−0.08	−0.03	0.03
Good's coverage	0.25	0.48	−0.00	0.26	0.01
Observed species	0.40	0.25	−0.05	−0.00	0.00
Pielou e	0.48	0.30	−0.18	0.09	0.14
Shannon	0.45	0.31	−0.17	0.06	0.13
Simpson	0.44	0.15	−0.13	0.06	0.10

TC: total carbon; TN: total nitrogen. C/N: total carbon/total nitrogen ratio. ** denotes a significant difference at the 0.01 level. * denotes a significant difference at the 0.05 level.
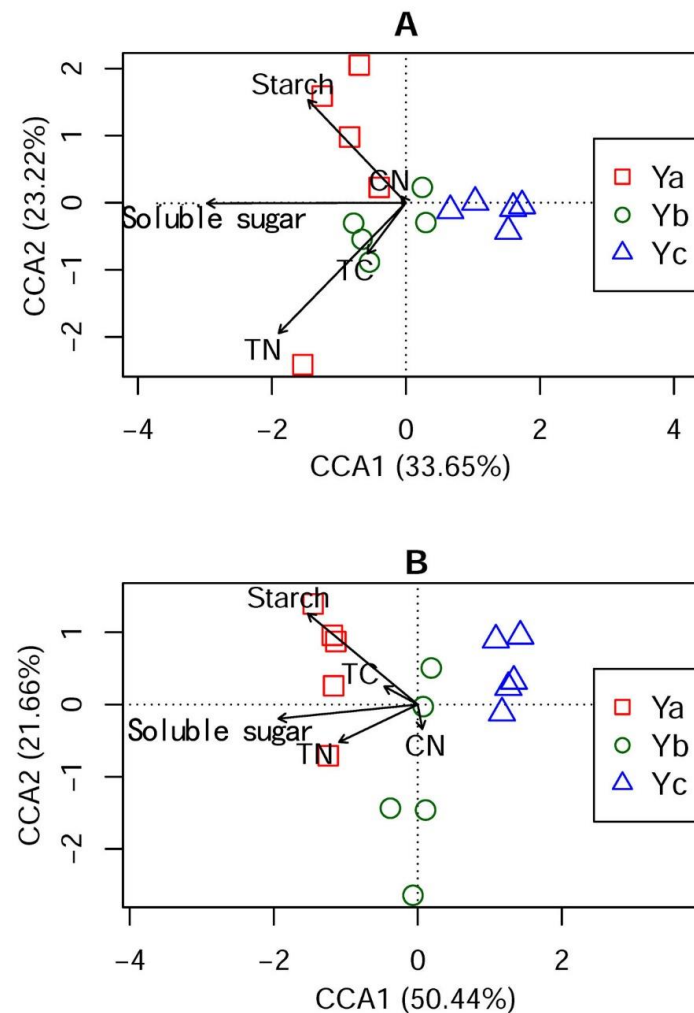
Figure 7. A canonical correlation analysis was used to illustrate the relationships between leaf characteristics and phyllosphere bacterial (**A**) and fungal (**B**) community composition. Ya: healthy *Pinus tabuliformis* trees; Yb: diseased *P. tabuliformis* trees at an early stage of *B. xylophilus* infection; Yc: diseased *P. tabuliformis* trees in the last stage. TC: total carbon; TN: total nitrogen; CN: total carbon/total nitrogen ratio.

4. Discussion and Conclusions

The microbiome has long been acknowledged as a crucial component of the plant ecosystem and is closely related to plant growth and disease resistance [39]. There is mounting evidence that plants under biotic or abiotic stress can use a variety of chemical cues to attract advantageous microbes or threats from the environment, improving their capacity to deal with the stress [12]. The phyllosphere microbiome, which is located aboveground, has received less research in recent years than the rhizosphere microbiome, which is located underground [27,40]. In the current study, we highlighted the phyllosphere microbiome shift, which could advance our understanding of the role of phyllosphere microbiome responses upon nematode infection challenge, and profiled the changes in the *P. tabuliformis* phyllosphere microbiome among healthy and infected by *B. xylophilus* under field conditions. Our results showed that the Chao 1 index and Shannon index significantly increased in infected leaves when compared to uninfected leaves (Tables 1 and 2), and new microbes (at ASV level) emerged in the infected leaves compared to the uninfected leaves, implying that only a limited number of microbiota members in the phyllosphere were involved in the response to infection.

The three main phyllosphere bacterial groups in our study were Proteobacteria, Bacteroidetes, and Actinobacteria. According to earlier research, Actinobacteria, Bacteroidetes, Firmicutes, and Proteobacteria make up the majority of the bacteria in the phyllosphere of plants [41]. The phyllosphere bacteria, classified as belonging to *Pantoea*, *Actinetobacter*, *Sphingomonas*, *Methylobacterium*, and *Pseudomonas*, were all discovered in previous studies [42], indicating that they were widespread in the phyllosphere of plants [43]. Each plant ecosystem contains a diverse microbial community that performs a variety of functions that may promote plant growth or act as biocontrol agents for nematode infection [29]. Actinobacteria were shown to have nematocidal activity in earlier studies [44–46]. Actinobacteria were relatively abundant in Yb and Yc in our study, indicating that bacteria associated with nematodes were essential for infection development [47,48]. Additionally, Yc had the highest levels of Stenotrophomonas, which was consistent with earlier studies [49,50]. We anticipated that pine wilt disease would have a significant impact on the host bacterial and fungal community structure because a prior study demonstrated that *B. xylophilus* infection can affect host microbial communities [13,14]. If you want to test this conjecture, it is recommended that the defense mechanisms of Actinobacteria and Stenotrophomonas should be further explored using molecular biology and metabolomics [51,52]. Our findings demonstrate that the phyllosphere bacterial and fungal microbial communities of the various treatments varied noticeably in terms of beta-diversity. From the results of the LEfSe, we found that Acidobacteria, Deinococcus-Thermus, Patescibacteria, Sphingoaurantiacus, and Amantichitinum were biomarkers of Yc (Figure 5B), suggesting that these bacteria are likely to help pine trees resist *B. xylophilus* infection. The defense mechanisms should be further explored using molecular biology and metabolomics. In order to promote resistance to nematode infection, plants can generally control nematode infection interactions or activate innate immune responses [53,54]. From our results, it can be inferred that *P. tabulaeformis* may change the phyllosphere bacterial community and select some biocontrol bacteria to improve plant resistance to *B. xylophilus*. Brevibacillus, Pseudomonas, and Bacillus are a few biocontrol bacteria groups that are prevalent and have antibiotic activities in the phyllosphere of *Arabidopsis thaliana* [24]. It is widely established that plants can selectively attract populations of helpful microbes that increase disease resistance and promote growth [55].

In addition to examining changes in microbial taxa, network inferences on changes in microbial interactions can offer further hints about how the microbiome affects plant health (Figure 6). Our research revealed that the bacterial-to-bacterial microbial network in the phyllosphere of infected leaves was more intense than that in uninfected leaves (Figure 6, Table 2). When microbes encounter environmental pressures, such as infection by the *B. xylophilus* nematode, highly connected networks, such as those in the infected leaves, can develop [56]. Additionally, earlier research suggested that the complex network

might lessen the success of *B. xylophilus* nematode invasion [57]. Our results thus point to a potentially positive function for the robust microbial networks seen in infected leaves.

A limiting factor for bacterial colonization in the phyllosphere is the availability of nutrients [58]. Leaves are the main source of nutrients, including carbohydrates, amino acids, and organic acids [59]. Additionally, the amount of nutrients is influenced by the plant species, genotype, and leaf characteristics such as the wettability, waxiness, and age [59]. A previous study found that lower leaf nitrogen concentrations were linked to more prevalent bacteria in the phyllosphere [59]. Additionally, there was a positive correlation between high leaf nitrogen and a high disease index, which may have been due to the nematode infection becoming more susceptible to nitrogen [43]. Our study found that TC and TN had relatively minor effects on the diversity of the microbial community, likely as a result of the lack of significant differences between TC and TN in the leaves of the three treatments (Table 1). The differences in phyllosphere microbial communities were mainly caused by the soluble sugar and starch contents of the leaves, a result that was consistent with the results of numerous previous studies [21,60]. The size of the overall bacterial population in the phyllosphere is known to be determined by sugars, which act as a limiting resource [61]. Our findings support a study that found that different plant species' leaves had varying degrees of influence on the structure of the bacterial community in the phyllosphere [19]. Our findings also demonstrated that leaf chemical characteristics shaped the bacterial community.

In conclusion, we propose that *B. xylophilus* infection of *P. tabulaeformis* trees caused changes in the physicochemical properties of leaves, leading to changes in phyllosphere microbial community composition and diversity. The soluble sugar and starch contents decreased based on the extent of infection, phyllosphere microbial community changes were potentially caused by *B. xylophilus* infection of *P. tabuliformis*, and the fungal community composition of Ya was clearly distinguished from Yb and Yc, especially along the first coordinate axis. Most of the microbial taxa tended to be co-excluding rather than co-occurring with the infection of PWD, especially in the last stage. These findings will significantly advance our understanding of the effects and mechanisms of *B. xylophilus* infection on alterations to phyllosphere microbial composition and diversity. Our study provides novel insights for understanding the roles of phyllosphere microbiome responses during pathogen challenge and their effect on plant health. It also provides phyllosphere evidence to support the "cry for help" strategy in plants. However, much work will be required to elucidate the different functions of the phyllosphere microbial communities in *B. xylophilus*-infected and *B. xylophilus*-uninfected trees.

References

1. Wang, Z.; Yang, H.; Wang, D.; Zhao, Z. Spatial distribution and growth association of regeneration in gaps of Chinese pine (*Pinus tabuliformis* Carr.) plantation in northern China. *Forest Ecol. Manag.* **2019**, *432*, 387–399. [CrossRef]
2. Kim, N.; Jeon, H.W.; Mannaa, M.; Jeong, S.I.; Kim, K.J.; Lee, C.; Park, A.R.; Kim, J.C.; Seo, Y.S. Induction of resistance against pine wilt disease caused by *Bursaphelenchus xylophilus* using selected pine endophytic bacteria. *Plant Pathol.* **2018**, *68*, 434–444. [CrossRef]
3. Futai, K. Pine wood nematode, *Bursaphelenchus xylophilus*. *Annu. Rev. Phytopathol.* **2013**, *51*, 61–83. [CrossRef]
4. Li, M.; Li, H.; Ding, X.; Wang, L.; Wang, X.; Chen, F. The detection of pine wilt disease: A literature review. *Int. J. Mol. Sci.* **2022**, *23*, 10797. [CrossRef]
5. Soliman, T.; Mourits, M.C.M.; van der Werf, W.; Hengeveld, G.M.; Robinet, C.; Lansink, G.M. Framework for Modelling Economic Impacts of Invasive Species, Applied to Pine Wood Nematode in Europe. *PLoS ONE* **2012**, *7*, e45505. [CrossRef] [PubMed]
6. Zhu, L.; Ye, J.; Negi, S.; Xu, X.; Wang, Z.; Ji, J. Pathogenicity of aseptic *Bursaphelenchus xylophilus*. *PLoS ONE* **2012**, *7*, e38095. [CrossRef]
7. Qiu, X.; Wu, X.; Huang, L.; Ye, J. Influence of Bxpel1 Gene Silencing by dsRNA Interference on the Development and Pathogenicity of the Pine Wood Nematode, *Bursaphelenchus xylophilus*. *Int. J. Mol. Sci.* **2016**, *17*, 125. [CrossRef]
8. Zhou, L.; Chen, F.; Xie, L.Y.; Pan, H.Y.; Ye, J.R. Genetic diversity of pine–parasitic nematodes *Bursaphelenchus xylophilus* and *Bursaphelenchus mucronatus* in China. *Forest Pathol.* **2017**, *47*, 4. [CrossRef]
9. Liu, K.; Ben, A.; Han, Z.; Guo, Y.; Cao, D. Interspecific hybridization between *Bursaphelenchus xylophilus* and *Bursaphelenchus mucronatus*. *J. For. Res.* **2019**, *30*, 699–707. [CrossRef]
10. Kawai, M.; Shoda-Kagaya, E.; Maehara, T.; Zhou, Z.; Lian, C.; Iwata, R.; Yamane, A.; Hogetsu, T. Genetic Structure of Pine Sawyer *Monochamus alternatus* (Coleoptera: Cerambycidae) Populations in Northeast Asia: Consequences of the Spread of Pine Wilt Disease. *Environ. Entomol.* **2006**, *35*, 569–579. [CrossRef]
11. Liu, H.; Brettell, L.E.; Qiu, Z.; Singh, B.K. Microbiome-mediated stress resistance in plants. *Trends Plant Sci.* **2020**, *25*, 733–743. [CrossRef] [PubMed]
12. Douanla-Meli, C.; Langer, E.; Mouafo, F.T. Fungal endophyte diversity and community patterns in healthy and yellowing leaves of Citrus limon. *Fungal Ecol.* **2013**, *6*, 212–222. [CrossRef]
13. Tian, B.; Cao, Y.; Zhang, K. Metagenomic insights into communities, functions of endophytes, and their associates with infection by root-knot nematode, Meloidogyne incognita, in tomato roots. *Sci. Rep.* **2015**, *5*, 17087. [CrossRef] [PubMed]
14. Vives-Peris, V.; Molina, L.; Segura, A.; Gómez-Cadenas, A.; Pérez-Clemente, R.M. Root exudates from citrus plants subjected to abiotic stress conditions have a positive effect on rhizobacteria. *J. Plant Physiol.* **2018**, *228*, 208–217. [CrossRef]
15. Cheng, X.; Cheng, F.; Xu, R.; Xie, B. Genetic variation in the invasive process of *Bursaphelenchus xylophilus* (Aphelenchida: Aphelenchoididae) and its possible spread routes in China. *Heredity* **2008**, *100*, 356–365. [CrossRef] [PubMed]
16. Xu, D.; Xu, L.; Zhou, F.; Wang, B.; Wang, S.; Lu, M.; Sun, J. Gut Bacterial Communities of *Dendroctonus valens* and Monoterpenes and Carbohydrates of *Pinus tabuliformis* at Different Attack Densities to Host Pines. *Front. Microbiol.* **2018**, *9*, 1251. [CrossRef] [PubMed]
17. Zhang, N.; Wang, D.; Liu, Y.; Li, S.; Shen, Q.; Zhang, R. Effects of different plant root exudates and their organic acid components on chemotaxis, biofilm formation and colonization by beneficial rhizosphere-associated bacterial strains. *Plant Soil* **2014**, *374*, 689–700. [CrossRef]
18. Hayat, S.; Faraz, A.; Faizan, M. Root Exudates: Composition and Impact on Plant–Microbe Interaction. In *Biofilms in Plant and Soil Health*; John Wiley & Sons: Hoboken, NJ, USA, 2017.
19. Yadav, R.K.; Karamanoli, K.; Vokou, D. Bacterial colonization of the phyllosphere of mediterranean perennial species as influenced by leaf structural and chemical features. *Microb. Ecol.* **2005**, *50*, 185–196. [CrossRef]
20. Kembel, S.W.; O'Connor, T.K.; Arnold, H.K.; Hubbell, S.P.; Wright, S.J.; Green, J.L. Relationships between phyllosphere bacterial communities and plant functional traits in a neotropical forest. *Proc. Natl. Acad. Sci. USA* **2014**, *111*, 13715–13720. [CrossRef]
21. Chen, T.; Nomura, K.; Wang, X.; Sohrabi, R.; Xu, J.; Yao, L.; Paasch, B.C.; Ma, L.; Kremer, J.; Cheng, Y.; et al. A plant genetic network for preventing dysbiosis in the phyllosphere. *Nature* **2020**, *580*, 653–657. [CrossRef]
22. Lexeau, J.H. A brief from the leaf: Latest research to inform our under-standing of the phyllosphere microbiome. *Curr. Opin. Microbiol.* **2019**, *49*, 41–49. [CrossRef]
23. Helfrich, E.J.N.; Vogel, C.M.; Ueoka, R.; Schäfer, M.; Ryffel, F.; Müller, D.B.; Probst, S.; Kreuzer, M.; Piel, J.; Vorholt, J.A. Bipartite inter-actions, antibiotic production and biosynthetic potential of the Arabidopsis leaf microbiome. *Nat. Microbiol.* **2018**, *3*, 909–919. [CrossRef] [PubMed]
24. Getzke, F.; Thiergart, T.; Hacquard, S. Contribution of bacterial-fungal balance to plant and animal health. *Curr. Opin. Microbiol.* **2019**, *49*, 66–72. [CrossRef]
25. Carrion, V.; Jaramillo, J.E.P.; Cordovez, V.; Tracanna, V.; de Hollander, M.; Ruiz-Buck, D.; Mendes, L.W.; van Ijcken, W.F.J.; Gomez-Exposito, R.; Elsayed, S.S.; et al. Pathogen-induced activation of disease-suppressive functions in the endophytic root microbiome. *Science* **2019**, *366*, 606–612. [CrossRef]
26. Yin, C.; Vargas, J.M.C.; Schlatter, D.C.; Hagerty, C.H.; Hulbert, S.H.; Paulitz, T.C. Rhizosphere community selection reveals bacteria associated with reduced root disease. *Microbiome* **2021**, *9*, 86. [CrossRef]

27. Sang, M.K.; Kim, K.D. Plant growth-promoting rhizobacteria suppressive to Phytophthora blight affect microbial activities and communities in the rhizosphere of pepper (*Capsicum annuum* L.) in the field. *Appl. Soil Ecol.* **2012**, *62*, 88–97. [CrossRef]

28. Zhou, J.; Deng, Y.; Luo, F.; He, Z.; Yang, Y. Phylogenetic Molecular Ecological Network of Soil Microbial Communities in Response to Elevated CO_2. *mBio* **2011**, *2*, e00122-11. [CrossRef]

29. Shi, C.; Wang, C.; Xu, X.; Huang, B.; Wu, L.; Yang, D. Comparison of bacterial communities in soil between nematode-infected and nematode-uninfected *Pinus massoniana* pinewood forest. *Appl. Soil Ecol.* **2015**, *85*, 11–20. [CrossRef]

30. Tóth, Á. *Bursaphelenchus xylophilus*, the pinewood nematode: Its significance and a historical review. *Acta Biologica Szegediensis* **2011**, *55*, 213–217.

31. Deckers, J.A.; Driessen, P.M.; Nachtergaele, F.; Spaargaren, O. The world reference base for soil resources. In *Soils of Tropical Forest Ecosystems Characteristics Ecology and Management*; Spinger: Berlin/Heidelberg, Germany, 2016; Volume 41, pp. 21–28.

32. Millberg, H.; Boberg, J.; Stenlid, J. Changes in fungal community of Scots pine (*Pinus sylvestris*) needles along a latitudinal gradient in Sweden. *Fung. Ecol.* **2015**, *17*, 126–139. [CrossRef]

33. Kikuchi, T.; Aikawa, T.; Oeda, Y.; Karim, N.; Kanzaki, N. A Rapid and Precise Diagnostic Method for Detecting the Pinewood Nematode *Bursaphelenchus xylophilus* by Loop-Mediated Isothermal Amplification. *Phytopathology* **2009**, *99*, 1365–1369. [CrossRef] [PubMed]

34. Ren, G.; Zhu, C.W.; Alam, M.S.; Tokida, T.; Sakai, H.; Nakamura, H.; Usui, Y.; Zhu, J.G.; Hasegawa, T.; Jia, Z.J. Response of soil, leaf endosphere and phyllosphere bacterial communities to elevated CO_2 and soil temperature in a rice paddy. *Plant Soil* **2015**, *392*, 27–44. [CrossRef]

35. Liu, J.; Ding, C.; Zhang, W.; Wei, Y.; Zhou, Y.; Zhu, W. Litter mixing promoted decomposition rate through increasing diversities of phyllosphere microbial communities. *Front. Microbiol.* **2022**, *13*, 1009091. [CrossRef] [PubMed]

36. Quast, C.; Pruesse, E.; Yilmaz, P.; Gerken, J.; Schweer, T.; Yarza, P.; Peplies, J.; Glöckner, F.O. The SILVA ribosomal RNA gene database project: Improved data processing and web-based tools. *Nucleic Acids Res.* **2013**, *41*, D590–D596. [CrossRef] [PubMed]

37. Kõljalg, U.; Nilsson, R.H.; Abarenkov, K.; Tedersoo, L.; Taylor, A.F.S.; Bahram, M.; Bates, S.T.; Bruns, T.D.; Bengtsson-Palme, J.; Callaghan, T.M.; et al. Towards a unified paradigm for sequence-based identification of fungi. *Mol. Ecol.* **2013**, *22*, 5271–5277. [CrossRef]

38. Segata, N.; Izard, J.; Waldron, L.; Gevers, D.; Miropolsky, L.; Garrett, W.S.; Huttenhower, C. Metagenomic biomarker discovery and explanation. *Genome Biol.* **2011**, *12*, R60. [CrossRef]

39. Cordovez, V.; Dini-Andreote, F.; Carrión, V.J.; Raaijmakers, J.M. Ecology and evolution of plant microbiomes. *Annu. Rev. Microbiol.* **2019**, *73*, 69–88. [CrossRef]

40. Kwak, M.; Kong, H.G.; Choi, K.; Kwon, S.; Song, J.Y.; Lee, J.; Lee, P.A.; Choi, S.Y.; Seo, M.; Lee, H.J.; et al. Rhizosphere microbiome structure alters to enable wilt resistance in tomato. *Nat. Biotechnol.* **2018**, *36*, 1100–1109. [CrossRef]

41. Bulgarelli, D.; Schlaeppi, K.; Spaepen, S.; van Themaat, E.; Schulze-Lefert, P. Structure and functions of the bacterial microbiota of plants. *Annu. Rev. Plant Biol.* **2013**, *64*, 807–838. [CrossRef]

42. Rastogi, G.; Coaker, G.L.; Leveau, J.H.J. New insights into the structure and function of phyllosphere microbiota through high-throughput molecular approaches. *FEMS Microbiol. Lett.* **2013**, *348*, 1–10. [CrossRef]

43. Jayakumar, J.; Ramakrishnan, S. Evaluation of Avermectin and its Combination with Nematicide and Bioagents against Root Knot Nematode, Meloidogyne incognita in Tomato. *J. Biol. Control* **2009**, *23*, 317–319. [CrossRef]

44. Anter, A.; Amin, A.; Ashoub, A.; El-Nuby, A. Evaluation of some rhizobacteria as induce systemic resistance or biocontrol agents in controlling root-knot nematode, Meloidogyne incognita on tomato. *Egypt. J. Agronematol.* **2014**, *13*, 107–123. [CrossRef]

45. Siddique, S.; Syed, Q.; Adnan, A.; Qureshi, F.A. Solation, Characterization and Selection of Avermectin-Producing Streptomyces avermitilis Strains from Soil Samples. *Jundishapur J. Microbiol.* **2014**, *7*, e10366. [CrossRef] [PubMed]

46. Zhao, L.; Mota, M.; Vieira, P.; Buycher, R.A.; Sun, J. Interspecific communication between pinewood nematode, its insect vector, and associated microbes. *Trends Parasitol.* **2014**, *30*, 299–308. [CrossRef]

47. Proença, D.N.; Grass, G.; Morais, P.V. Understanding pine wilt disease: Roles of the pine endophytic bacteria and of the bacteria carried by the disease-causing pinewood nematode. *Microbiologyopen* **2017**, *6*, e00415. [CrossRef]

48. Xiang, Y.; Wu, X.; Zhou, A. Bacterial Diversity and Community Structure in the Pine Wood Nematode *Bursaphelenchus xylophilus* and *B. mucronatus* with Different Virulence by High-Throughput Sequencing of the 16S rDNA. *PLoS ONE* **2015**, *10*, e0137386. [CrossRef]

49. Proença, D.; Francisco, R.; Santos, C.V.; Lopes, A.; Fonseca, L.; Abrantes, I.M.O.; Morais, P.V. Diversity of bacteria associated with *Bursaphelenchus xylophilus* and other nematodes isolated from *Pinus pinaster* trees with pine wilt disease. *PLoS ONE* **2010**, *5*, e15191. [CrossRef] [PubMed]

50. Millet, Y.A.; Danna, C.H.; Clay, N.K.; Songnuan, W.; Simon, M.D.; Werck-Reichhart, D.; Ausubel, F.M. Innate immune responses activated in Arabidopsis roots by microbe-associated molecular patterns. *Plant Cell* **2010**, *22*, 973–990. [CrossRef]

51. Zdouc, M.M.; Iorio, M.; Maffioli, S.I.; Crüsemann, M.; Donadio, S.; Sosio, M. Planomonospora: A Metabolomics Perspective on an Underexplored Actinobacteria Genus. *J. Nat. Prod.* **2021**, *84*, 204–219. [CrossRef]

52. Alexander, A.; Singh, V.K.; Mishra, A. Overexpression of differentially expressed AhCytb6 gene during plant-microbe interaction improves tolerance to N_2 deficit and salt stress in transgenic tobacco. *Sci. Rep.* **2021**, *11*, 13435. [CrossRef]

53. Innerebner, G.; Knief, C.; Vorholt, J.A. Protection of Arabidopsis thaliana against leaf-pathogenic *Pseudomonas syringae* by Sphingomonas strains in a controlled model system. *Appl. Environ. Microbiol.* **2011**, *77*, 3202–3210. [CrossRef]

54. Mendes, L.W.; Raaijmakers, J.M.; de Hollander, M.; Mendes, R.; Tsai, S.M. Influence of resistance breeding in common bean on rhizosphere microbiome composition and function. *ISME J.* **2018**, *12*, 212–224. [CrossRef]

55. Faust, K.; Raes, J. Microbial interactions: From networks to models. *Nat. Rev. Microbiol.* **2012**, *10*, 538–550. [CrossRef] [PubMed]

56. Wei, Z.; Gu, Y.; Friman, V.; Kowalchuk, G.A.; Xu, Y.; Shen, Q.; Jousset, A. Initial soil microbiome composition and functioning predetermine future plant health. *Sci. Adv.* **2019**, *5*, eaaw0759. [CrossRef]

57. Remus-Emsermann, M.N.P.; Schlechter, R.O. Phyllosphere microbiology: At the interface between microbial individuals and the plant host. *New Phytol.* **2018**, *218*, 1327–1333. [CrossRef] [PubMed]

58. Tukey, J.H.B. The Leaching of Substances from Plants. *Annu. Rev. Plant. Physiol.* **1970**, *21*, 305–324. [CrossRef]

59. Laforest-Lapointe, I.; Messier, C.; Kembel, S.W. Host species identity, site and time drive temperate tree phyllosphere bacterial community structure. *Microbiome* **2016**, *4*, 27. [CrossRef] [PubMed]

60. Delmotte, N.; Knief, C.; Chaffron, S.; Innerebner, G.; Roschitzki, B.; Schlapbach, R.; von Meing, C.; Vorholt, J.A. Community proteogenomics reveals insights into the physiology of phyllosphere bacteria. *PNAS* **2009**, *106*, 16428–16433. [CrossRef]

61. van der Wal, A.; Leveau, J.H.L. Modelling sugar diffusion across plant leaf cuticles: The effect of free water on substrate availability to phyllosphere bacteria. *Environ. Micrbiol.* **2011**, *13*, 792–797. [CrossRef]